



Light-Induced Transcription Activation for Time-Lapse Microscopy Experiments in Living Cells

Jorge Trojanowski, Anne Rademacher, Fabian Erdel, and Karsten Rippe

Abstract

Gene expression can be monitored in living cells via the binding of fluorescently tagged proteins to RNA repeats engineered into a reporter transcript. This approach makes it possible to trace temporal changes of RNA production in real time in living cells to dissect transcription regulation. For a mechanistic analysis of the underlying activation process, it is essential to induce gene expression with high accuracy. Here, we describe how this can be accomplished with an optogenetic approach termed blue light-induced chromatin recruitment (BLInCR). It employs the recruitment of an activator protein to a target promoter via the interaction between the PHR and CIBN plant protein domains. This process occurs within seconds after setting the light trigger and is reversible. Protocols for continuous activation as well as pulsed activation and reactivation with imaging either by laser scanning confocal microscopy or automated widefield microscopy are provided. For the semiautomated quantification of the resulting image series, an approach has been implemented in a set of scripts in the R programming language. Thus, the complete workflow of the BLInCR method is described for mechanistic studies of the transcription activation process as well as the persistence and memory of the activated state.

Key words Optogenetics, Transcription dynamics, Automated microscopy, Image quantification

1 Introduction

Following reporter RNAs in living cells over time by fluorescence light microscopy imaging has provided valuable information on gene regulation and RNA processing [1–5]. In these experiments RNA is visualized by fluorescently tagged RNA binding proteins that recognize specific secondary structures engineered into the transcript like MS2 or PP7 motifs [6, 7]. Transcription is frequently induced via the doxycycline (dox)-dependent binding of activator protein fusions with bacterial tetracycline repressor (TetR) to its high-affinity operator (*tetO*) sites integrated at the promoter

Electronic supplementary material: The online version of this chapter (https://doi.org/10.1007/978-1-4939-9674-2_17) contains supplementary material, which is available to authorized users.

[8, 9]. However, the start point of this reaction depends on the permeation times of dox and the association kinetics of TetR. This process occurs over a time interval of at least several minutes, which confounds the analysis of early transcription kinetics. To circumvent this problem light-induced uncaging of an inducer molecule has been reported [4]. Yet it does not overcome the limitation that this type of chemical induction cannot be reversed quickly. While the inducer can be removed by repeated washing steps, the resulting dissociation times are well above the minute timescale, which makes it difficult to analyze the effect of a temporally limited activation stimulus. The above-described issues can be addressed by taking advantage of optogenetic approaches as for example the light-induced heterodimerization of the plant PHR and CIBN protein domains [10]. We recently developed a PHR-CIBN based optogenetic system termed blue light-induced chromatin recruitment (BLInCR) that combines rapid and reversible light-dependent recruitment of effector proteins with a real-time readout for transcription [11] (Fig. 1a). The human osteosarcoma cell line U2OS 2-6-3 used in these experiments has been developed previously in the Spector lab [9]. It consists of a tandem array of ~200 copies of a reporter gene. This reporter has *lacO* and *tetO* repeats in proximity to a minimal CMV promoter. Activator binding to the *tetO* sites induces transcription of a reporter RNA, which contains binding sequences for the MS2 coat protein (MCP) and encodes for peroxisome-targeted cyan fluorescent protein (CFP) (Fig. 1b). In this model system, transcription factor binding to the *tetO* sites via PHR-CIBN interactions can be controlled with high temporal precision in living cells, while RNA production is traced via tagging the MS2 reporter RNA with fluorescently labeled MCP [11]. Due to the presence of multiple integration sites, transcription factor binding and dissociation as well as RNA production can be visualized by fluorescence microscopy in single cells using conventional confocal or widefield systems (Fig. 1c, d). Related approaches have been introduced by other groups and include targeting of endogenous genes by light-induced TALEs [12], bacterial light-induced transcription factors [13, 14] and targeting light-recruited activators to dCas9 [15].

Here, we provide protocols for conducting experiments with the BLInCR system and for a semiautomated quantification of the resultant image series with a set of scripts written in the R programming language [16]. In one type of experiments continuous blue light illumination and persistent activation is employed. The other approach described here uses pulsed activation and reactivation after an intermittent period without a light trigger during which the activator dissociates. Furthermore, image acquisition protocols for either widefield or confocal microscopy are presented. The higher spatial resolution of the confocal imaging mode allows to resolve heterogeneities inside the transcription locus (Fig. 1c). In

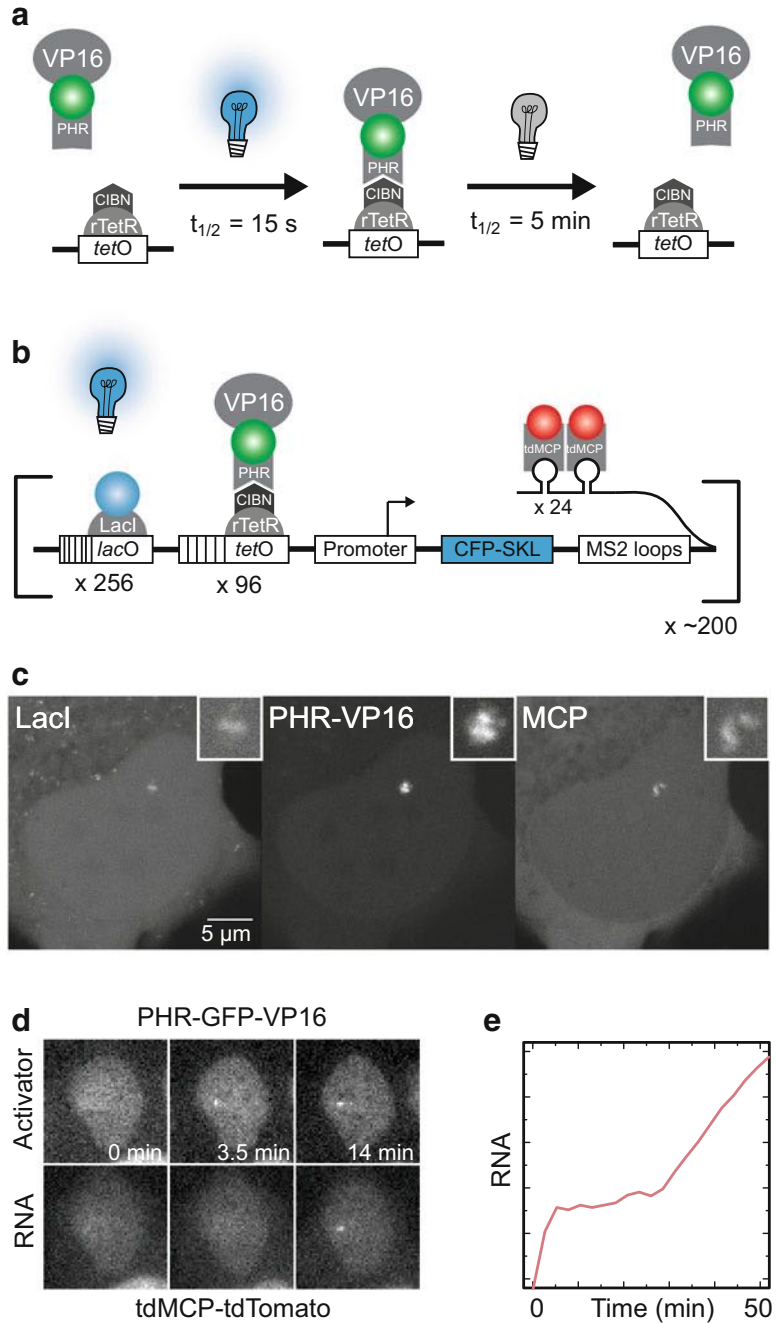


Fig. 1 Application of BLInCR for light-induced transcription activation. **(a)** Upon blue light illumination the PHR domain switches its conformation in the PHR-GFP-VP16 construct and binds to CIBN fused to rTetR (CIBN-rTetR). In the presence of dox, rTetR is bound to DNA via the *tetO* sequence. This leads to the fast recruitment of the VP16 transcription activator with $t_{1/2} = 15 \text{ s}$ [11]. If the blue light is switched off, dissociation occurs ($t_{1/2} = 5 \text{ min}$). **(b)** Transfecting the U2OS 2-6-3 cell line with CIBN-rTetR and PHR-GFP-VP16 allows direct

addition, illumination and activation are restricted to the imaged area. For imaging larger cell numbers (e.g., for resolving the cell-to-cell heterogeneity of transcription activation kinetics), the application of widefield microscopy can be advantageous (Fig. 1d). Quantification of the time-lapse image series obtained in these experiments with the set of R-scripts provided yields RNA production kinetics (Fig. 1e), from which information on the underlying mechanism is obtained [11]. The protocols can be easily applied to study the effects of transcriptional inhibitors or to evaluate via repeated activation cycles if the activated promoter state is “memorized” and how long it persists in the absence of the activator. Furthermore, we envision that our experimental approach will prove to be useful for a variety of other applications that require temporal precision and/or reversibility, for example, inducing DNA damage response by increasing the local concentration of damage factors [17] or perturbing the epigenetic landscape by recruiting modifiers [18].

2 Materials

2.1 Cell Culture

1. Reporter cell line, for example U2OS 2-6-3 [9] (*see Note 1*).
2. Cell culture slide suited for fluorescence microscopy (e.g., 8-well chambered cover glass No. 1 borosilicate, Nunc Labtek).
3. Complete medium: DMEM medium (1 g/L glucose) without phenol-red supplemented with 10% tetracycline-free fetal calf serum (FCS), penicillin/streptomycin, 2 mM L-glutamine.
4. Phosphate-buffered saline (PBS).
5. 0.05% trypsin–0.02% EDTA in PBS.
6. Doxycycline, 1 mg/mL in water.

Fig. 1 (continued) measurements of light-induced promoter activity. The cell line contains approximately 200 copies of a stably integrated reporter construct with a minimal CMV promoter under the control of 256 *lacO* and 96 *tetO* repeats [9]. The nascent RNA contains MS2-stem loops that are bound by fluorescently tagged MCP (tdMCP-tdTomato) and additionally encodes CFP-SKL as a fluorescent protein reporter localized to peroxisomes. The locus can additionally be labeled by fluorescently tagged LacI. **(c)** Confocal microscopy allows to assess the structure of the transcription site in addition to its intensity. The array was labeled by CFP-LacI. The PHR-YFP-VP16 fusion protein was recruited to CIBN-TetR upon blue light illumination and nascent RNA was labeled via binding of MCP-mKate2. **(d)** Widefield image series of activator recruitment and onset of transcription. **(e)** Kinetics of RNA production at the reporter array obtained from quantification of a time-lapse image series

7. Opti-MEM medium.
8. Transfection reagent (e.g., Xtreme Gene 9, Roche).
9. Colored, nontransparent polystyrene foam box (*see* **Note 2**).

2.2 Plasmids (*See Note 3*)

Plasmid selection with respect to the fluorescent protein (FP) that is used to visualize the respective constructs is critical for the experiment and depends on the type of activation pattern that is desired. Examples of fluorophore combinations for continuous activation and pulsed activation and reactivation are summarized in Table 1.

1. A fluorescently tagged transcription activator fused to PHR (pPHR-GFP-NLS-VP16, pPHR-YFP-NLS-VP16 (Addgene #103821) or for reversibility studies pPHR-iRFP713-NLS-VP16 (Addgene #103823), which has a far-red label and can be monitored without triggering recruitment).
2. A fluorescently tagged negative control effector (pPHR-GFP-NLS or pPHR-YFP-NLS, Addgene #103817).
3. A *tetO*-directed localizer (pCIBN-rTetR: reverse TetR, which binds in the presence of dox; or pCIBN-TetR (Addgene #103813): TetR, which binds in the absence of dox, *see* **Note 4**).
4. Fluorescently tagged MS2 RNA reader (pCMV Δ TATA-tdMCP-tdTomato, *see* **Note 5** or mKate2-MS2, Addgene #103833).

Table 1
Exemplary fluorophore combinations for continuous and pulsed activation patterns

Experiment	Protein domain(s)	Coupled FP	Excitation (nm)	Emission (nm)
Continuous activation	Activator (PHR-VP16)	GFP/YFP	488	500–550
	Localizer (CIBN-rTetR, fluorescent label optional)	tagBFP/CFP ^a	405	415–475
	RNA reader (MCP)	mKate2 or tdTomato	561/594 ^b	605–750
	Array marker (LacI, optional)	tagBFP/CFP ^a	405	415–475
Pulsed activation with dissociation of activator	Activator (PHR-VP16)	iRFP713	633	645–780
	Localizer (CIBN-rTetR) ^c	GFP/YFP	488	500–550
	RNA reader (MCP)	tdTomato	561	570–615
	Array marker (LacI, optional) ^c	GFP/YFP	488	500–550

The above fluorophore combinations worked well in terms of spectral separation of the different FPs and recruitment of light-dependent constructs while imaging. Excitation with 405 nm or 488 nm induces the PHR-CIBN interaction

^aFluorescent labeling the TetR localizer or LacI binding to the *lacO* sites in the U2OS 2-6-3 cell line as an additional array marker is optional. One of the two proteins can be tagged with a blue fluorophore as indicated in the table. However, the choice of color will depend on the specific application. A red color needs to be chosen if it is necessary to decouple visualization of bound TetR or LacI from the light-induced PHR-CIBN interaction

^bExcitation worked better at 561 nm, but less bleaching was observed at 594 nm

^cTo reliably localize the reporter array either a fluorescently labeled CIBN-rTetR or LacI construct can be used

5. Optional: an additional reporter array marker (e.g., tagBFP-LacI, Addgene #103839).

2.3 Microscope

For recording high resolution images and time series of single cells, a laser scanning confocal fluorescence microscope with appropriate image acquisition software is recommended. We have used a Leica SP5 with the Leica application suite advanced fluorescence (LAS AF) software that was equipped with the following parts:

1. A 63× oil objective (e.g., HCX PL APO lambda blue 63×/1.40 oil UV objective).
2. A 488 nm laser to trigger recruitment and to image YFP- or GFP-tagged effector constructs.
3. A 561 or 594 nm laser to image red fluorescent constructs (e.g., tdTomato, mKate2) without triggering recruitment.
4. Optional: a 633 nm laser to image iRFP713-tagged effectors without triggering recruitment.
5. Optional: a UV laser diode to record additional constructs in the blue channel (e.g., tagBFP-LacI as an additional array marker).
6. A live cell incubation chamber that can be protected from light.
7. A red flashlight or LED to mount samples on the microscope without triggering recruitment. A removable bike tail light works well for this purpose.

For automated image acquisition of a larger number of cells, a fluorescence widefield microscope can be advantageous. For this purpose, we used a Zeiss AxioObserver Z1 with the ZEN 2012 pro software with modules for z-stack, time-lapse, multiposition, and heterogeneous acquisition and the following features:

1. Live cell incubation chamber (preferentially with black walls and a curtain for the front side).
2. Motorized stage.
3. Motorized z-drive.
4. Hardware or software autofocus.
5. Red filter for transmitted light.
6. Software with automation capabilities including time course and tile pattern (or grid) acquisition.
7. 20× air objective (e.g., Zeiss Plan-Apochromat 20x/0.8 M27).
8. Fluorescence lamp (e.g., mercury short arc reflector lamp HXP 120 V).

9. Filter sets (wavelength windows in nm for excitation, dichroic, emission): modified Cy3 filter (535/30, 570, 572/25) for tdTomato, GFP filter (470/40, 495, 525/40).

2.4 Software

1. R (version 3.2.3) [16].
2. RStudio (version 1.0.136) [19].
3. R packages: EBImage (version 4.12.2) [20], plyr (version 1.8.4) [21] and ggplot2 (version 3.1.0) [22].
4. R-package NSSQ “Nuclear Spot Segmentation and Quantification” available in the Supplementary Materials on the book webpage.
5. The Fiji distribution [23] of ImageJ [24] for general purpose image analysis.

3 Methods

3.1 Cell Culture (Days 0 and 1)

U2OS 2-6-3 cells [9] are maintained at standard cell culture conditions (37 °C and 5% CO₂) and split (1:6 to 1:10) every 2–3 days. They can be frozen in DMEM supplemented with 10% DMSO and 40% FCS.

1. On day 0, seed cells in the 8-well slide in 400 μL medium at a density of $2 \cdot 10^4$ per well. After adding the cell suspension to wells, let the slide stand for 5–10 min to obtain a homogeneous attachment of cells before transferring it to the incubator.
2. On day 1, replace growth medium with a reduced volume (300 μL) and prepare transfection mix according to the manufacturer’s guidelines in a low binding tube. For a transcription activation experiment as depicted in Fig. 1, cotransfect cells with, for example, pPHR-GFP-VP16 (effector), pCIBN-rTetR (localizer), and pCMVΔTATA-tdMCP-tdTomato (RNA reader). As a negative control, use the mock effector plasmid pPHR-GFP-NLS instead of pPHR-GFP-VP16. When using Xtreme Gene 9 (Roche), use 20 μL Opti-MEM, 200 ng plasmid mixture (67 ng of each), and 0.6 μL reagent. Place the slide in a lightproof polystyrene foam box for later transport before returning it to the incubator. The lid should be placed on the box lightly to allow air exchange.

3.2 Time-Lapse Microscopy for Continuous Induction (Day 2)

In continuous induction experiments, cells are exposed to blue light during the whole acquisition time resulting in a constant high concentration of activator at the promoter. In the following section, two imaging modes are described. If a high spatial resolution is needed, confocal microscopy (Subheading 3.2.1) is advantageous. If large cell numbers are to be acquired, automated widefield microscopy is recommended (Subheading 3.2.2). Avoid blue/

white light exposure of the samples and use only red light during handling of the samples before induction.

1. Heat the microscope incubation chamber to 37 °C and wait for the temperature to stabilize (1–2 h).
2. When using the rTetR system, add dox to the well to be imaged at a final concentration of 5 µg/mL before each time-lapse acquisition. Wait at least 10 min to allow for CIBN-rTetR binding to the *tetO* array (*see* **Notes 4** and **6**).
3. Transfer the slide onto the microscope. Cover transparent walls of the incubation chamber with a dark cloth or aluminum foil.

3.2.1 Imaging by Confocal Microscopy

By confocal microscopy the spatial distribution of RNA at the array can be assessed, which is generally not homogeneous (Fig. 1c). In addition, the confocal microscopy setup can be extended to an analysis in three dimensions for data acquisition and quantification (e.g., as in [25]) to detect subtle intensity or shape changes over time. To reduce photobleaching by continuous laser exposure, cells can be exposed to blue light at regular intervals (2–3 min) that are shorter than the reversibility half-life time of the PHR-CIBN interaction (4.9 ± 0.8 min [11]) (*see* **Note 7**).

1. Locate cells in the red channel.
2. Record a prerecruitment stack of the RNA reader signal (excitation at 561/594 nm) to ensure that no premature activation has occurred. The latter can happen due to premature light exposure during cell preparation or transport. Select a laser intensity that yields a satisfactory signal-to-noise ratio for the time course recording. Typical imaging parameters are 512×512 pixel image size, zoom factor 9 corresponding to 53 nm/pixel, 400 Hz scan speed, $4\times$ line average, and 5–8 *z*-slices spaced 0.5 µm apart. Reducing the line average and minimizing the laser intensities can help to reduce photobleaching.
3. Record a stack of the effector (excitation at 488 nm), which will induce recruitment to the *tetO*-tethered localizer. For **Steps 2** and **3** a single multichannel stack can be recorded by choosing the option to switch between stacks with the stack in the red channel being recorded first.
4. Record two-channel stacks of the RNA reader and the effector every 2–3 min for about 45–60 min (*see* **Note 8**). Switching the channels between lines (as opposed to between slices or stacks) ensures that the images of the different channels are not shifted with respect to one another.
5. Optional: include a third channel for an additional array marker (e.g., tagBFP-LacI) or a second chromatin feature probe (e.g., a histone acetylation reader domain).

3.2.2 Automated Imaging by Widefield Microscopy

Widefield microscopy to monitor the onset of transcription is advantageous when assessing cell-to-cell heterogeneity of activation kinetics from the analysis of tens to hundreds of cells. In addition, photobleaching is reduced due to reduced light exposure, which is particularly relevant for longer time course experiments.

1. In a well that will not be used for data acquisition, define and test the acquisition pattern. Recommended starting values for acquisition parameters can be found in Table 2. Locate the cells in the transmission channel with a red filter at a central position in the well with a high density of cells (*see Note 9*).
2. Exposure times of the fluorescence channels for each channel should be chosen between 70 and 500 ms so that there are no saturated pixels while detecting most transfected cells.

Table 2
Recommended imaging parameters for widefield microscopy

Parameter	Range	Start value	Lower limit	Upper limit
Exposure time	70–500 ms	150 ms	ROI detection, maximum camera frame rate	Photodamage, detector saturation, throughput
Filter bandwidth	tdTomato: 535/30, 570, 572/25; GFP: 470/40, 495, 525/40		n.a.	n.a.
Intensity	Power 2–3 mm above objective: GFP: 1–2 mW, 488 nm tdTomato: 4–5 mW, 561 nm		ROI detection	Photodamage, formation of PHR aggregates
Sampling interval	1–7 min	3.5 min	Photodamage, throughput	Time resolution
Number of z-slices	3–5	3	Object size, z-drift, cell movements	Photodamage, acquisition time
z-Slice distance	0.3–2.0 μm	1.0 μm ($\times 20$ objective)	Height of z-stack and number of slices	z-extension of transcription spot
Number of positions	15–30	25	Throughput	Sampling frequency
Camera binning	1 \times 1 to 2 \times 2	2 \times 2	Signal intensity and noise	Spatial resolution of ROI
Objective magnification	$\times 20$ – $\times 60$	$\times 20$	Spatial resolution of ROI	Field of view, throughput

Imaging parameters and their recommended values refer to the microscope used here (Zeiss AxioObserver Z1). These need to be adjusted to account for the specific features of a given microscopy systems with respect to filters, fluorescence excitation source and camera. In addition to premature activation of PHR as described above, cross-talk between the different channels needs to be avoided

The *z*-stacks should have three slices and a distance between 0.8 and 1.5 μm depending on the axial resolution. Switch on the hardware focus, if available, or define a software autofocus routine for each position in the Cy3 channel (e.g., 25 μs exposure, 2×2 binning, 0.8 μm distance over 8.0 μm). Define a grid pattern of subpositions around the selected position. The number of subpositions in this pattern and the time required to image one position determine the sampling frequency. If acquisition of one position requires 8 s, 25 positions can be imaged once every 3.5 min. In the time course menu set the cycle interval to its minimal value and the experiment duration to 90 min. The order of acquisition should be first *z*-stacks, then channels, positions and time points. Acquiring the *z*-stack before switching channels increases acquisition speed. Activate autosaving of images in the tif file format.

3. If the first cycles of the test run yield focused images with a sufficient signal-to-noise ratio, move to a new well, wait 15 min, add dox, wait 15 min (*see Note 6*), select a good location as above, set the *z*-position and start the experiment.

3.3 Time-Lapse Microscopy for Pulsed Induction

Light-dependent transcription activation is particularly useful to assess the persistence of the activated state after dissociation of the activator from the promoter and the response of the promoter to subsequent reactivation. For this type of experiments, the activator (VP16) and the RNA reader (MCP) need to be visualized without triggering recruitment. Therefore, they can be tagged with two spectrally distinct red fluorophores such as iRFP713 and tdTomato. To locate the array, an array marker such as GFP-LacI or a fluorescent localizer (e.g., CIBN-YFP-TetR, Addgene #103798) should be used. These combinations of fluorescent proteins can be imaged on a confocal microscope with the appropriate laser lines (Subheading 3.3.1). For acquiring larger numbers of cells on a widefield microscope, we describe a simplified version of the reactivation protocol without imaging in the intermittent dark phase (Subheading 3.3.2).

3.3.1 Imaging by Confocal Microscopy

The imaging workflow described in Subheading 3.2.1 is adjusted as follows:

1. Record a two-channel (excitation at 561 and 633 nm) prerecruitment stack with the same typical imaging parameters as described above.
2. Record the desired pattern of three-channel stacks (excitation at 488, 561 and 633 nm) and two-channel stacks (561 and 633 nm) to cause activator association and dissociation, respectively. Exemplary illumination pattern (as in [11], stack recordings approximately 3 min apart): $1 \times$ prerecruitment, $2 \times$ recruitment, $12 \times$ without recruitment (i.e., approximately 40 min without blue light illumination), $5 \times$ rerecruitment.

3.3.2 Automated Imaging by Widefield Microscopy

With the combinations of fluorescent proteins and filter sets used here for widefield microscopy, image acquisition will lead to blue light exposure and activation. Accordingly, it is recommended to conduct two consecutive activation time courses with an intermittent delay for a dark phase without imaging. The continuous activation workflow described in Subheading 3.2.2 is modified, as follows:

1. Transfer cells to the microscope and test imaging settings in one well as described in Subheading 3.2.2.
2. Activate an irregular protocol setup (e.g., multiblock execution in the Zeiss Zen software).
3. Define two consecutive time course jobs of 60 min with 3.5 min intervals. Add a delay for the execution of the second job of the desired duration for the dark period.
4. Move to a new well, wait 15 min, add dox, find and set focus, wait 15 min for rTetR-binding and start the experiment (*see Note 6*).

3.4 Image Analysis

The experiments described above result in time series of multichannel, multislice image stacks (Leica SP5 confocal microscope) or image files in the tif file format (Zeiss widefield microscope). The Fiji distribution of ImageJ can be used for a general assessment of the images. In the following subsections, an approach for the intensity-based quantification of RNA levels is summarized according to the general workflow depicted in Fig. 2.

3.4.1 Low Throughput Analysis of Confocal Images

A typical transcription activation experiment recorded with a confocal microscope contains 15–25 multichannel, multislice image stacks. The analysis described below is a manual analysis using the Fiji distribution of ImageJ. It can be automated to some extent by using ImageJ macros, which is not discussed here.

1. Optional: If necessary, transform each multichannel *z*-stack to an RGB stack and register the slices using the TurboReg plugin for ImageJ [26] (*see Note 10*). The registration should be based on the effector or an array marker channel and use one of the central slices as a reference.
2. Create maximum intensity projections (Image → Stacks → Z Project...) resulting in multichannel images for each time point.
3. Select a sufficiently large circular region of interest (20–40 px) around the array and measure the mean fluorescence intensities (Analyze → Measure) in that ROI for all channels (effector, reader, and possibly array marker).
4. Select a reference region within the nucleus and measure its mean fluorescence intensity.

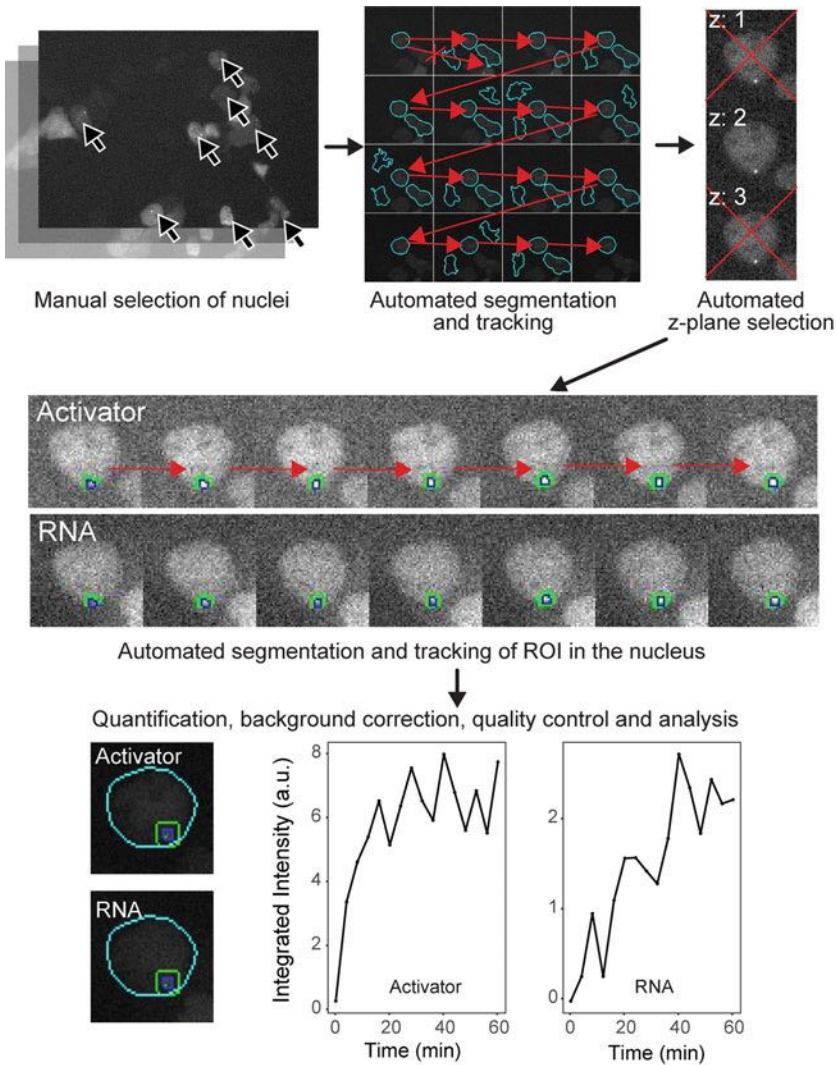


Fig. 2 Workflow for semiautomated transcription spot tracking and quantification. The analysis of an image series comprises a sequence of manual and automated steps. A typical experiment with image acquisition using a widefield microscope results in images for two channels, three z-planes, 16 time points, and 25 grid positions. For each grid position one image out of several z-positions, channels, and time frames is displayed to manually select nuclei. Selected nuclei are segmented and tracked and for each time point the optimal z-position is selected. The array spot is segmented, tracked, and used for intensity and area measurements. After manual quality control of the segmentation and tracking in the RNA channel, the single cell time course data can be visualized and used for further analysis or interpretation

5. Select a background region outside of the cell and measure its mean fluorescence intensity.
6. Repeat **steps 3–5** for each time point. Note that the array ROI should have the same size for the analysis of one cell.

7. Extract the time information for each multichannel, multislice stack from the metadata and calculate time points with respect to the first blue light exposure.
8. Account for bleaching by fitting the mean intensity difference between the nuclear reference region and the background region ($I_{\text{ref}}(t) - I_{\text{back}}(t)$) to an exponential decay ($I_{\text{ref}}(t) - I_{\text{back}}(t) = a \cdot e^{-k \cdot t}$).
9. Calculate the bleach-corrected RNA enrichment as $E(t) = (I_{\text{array}}(t) - I_{\text{ref}}(t)) / e^{-k \cdot t}$.
10. Optional: For averaging RNA enrichment time courses of different cells, interpolate enrichment values at regular time points for each cell ($E(0 \text{ min})$, $E(3 \text{ min})$, $E(6 \text{ min})$, etc.).

3.4.2 Semiautomated Image Analysis of Widefield Images

The semiautomated image analysis consists of four steps separated into four scripts: (1) manual selection of nuclei that show recruitment, (2) automated segmentation, tracking, and intensity quantification of nuclei and spots at the selected positions, (3) manual quality control of segmentation and tracking, and (4) summary and visualization of results. Example scripts are provided in the supplementary materials. The analysis workflow is summarized in Fig. 2. The image analysis is performed in R [16] and RStudio [19] and is based on the EBImage package [20]. We provide additional functions for segmentation and tracking of nuclei and spots with the NSSQ “Nuclear Spot Segmentation and Quantification” package. Details of the analysis workflow are included with the example scripts and can be found in the help pages of the NSSQ package. Parameters for segmentation and tracking are specified in the head section of the second script and may need adjustment for images acquired with different microscope settings.

1. Download the NSSQ package from the supplementary material on the book webpage. Install the package in R: `install.packages('./DownloadFolder/NSSQ_1.0.tar.gz', repos = NULL, type = "source")`.
2. Run the manual selection function in the first script using images of all grid positions in the central z -slice at frame 3 ($t = 7 \text{ min}$, where spots of recruited PHR-effector should have appeared) in the PHR-FP-effector channel (*NSSQ:select-Positions*). Images of the grid positions are displayed in the plot panel of RStudio. In each image, select nuclei with normal morphology showing recruitment of PHR-FP-effector and confirm the selection in the console. “s”: save selection and stay in this image to select more, “f”: save selection and move on to the next image, “n”: delete the selection and move on to the next image, “d”: delete selection, but stay in image. Save the position list.

3. In the second script, load the position list. Cycle over the entries of the position list and process each image region as follows.
4. Load the cropped image region in all channels for the central z -slice (*NSSQ: readImageRegion*). Cropping around the selected coordinates reduces the amount of data loaded into the working memory.
5. Segment nuclei using local thresholding and indicating the range of expected nuclei radii in pixel units (*NSSQ: thres_rad_border*). Then filter out nuclei outside the expected radius range (*NSSQ: filterObjects*).
6. For the tracking of the selected nucleus, determine the xy -coordinates of nuclei (*EImage: computeFeatures.moment*) first and then track forward and backward in time starting from frame 3, in which the nucleus has been manually selected (*NSSQ: twoWayTrack*). Use the tracking information and the xy -information for cropping of the nucleus in all channels (*NSSQ: cropMovingObjects*) and in the mask image.
7. For each frame, select the best z -position: Load the additional z -slices in all channels and crop according to the tracking information obtained above. Determine the best focus position (*NSSQ: selectInFocus*) and recompose the image series in all channels using the best-focus slice for each time point. Save the resulting image series and the nucleus mask.
8. Segment the reporter array spot inside the nuclear area in the PHR-FP-effector channel using the 99.5% intensity quantile for thresholding (*NSSQ: spot_segment*). Filter spots by their expected size indicating the minimum and maximum expected area in square-pixels.
9. Track the brightest spot. In order to reduce the computation time, first reduce the number of spots in each frame by excluding spots outside the time-projected main spot object (*NSSQ: projectionTracking*). Then track the main spot by minimizing the Euclidean distance of position and shape features between consecutive frames (*NSSQ: selectMainSpot*).
10. Repeat **steps 8** and **9** with decreasing thresholding quantiles until segmentation and tracking over a maximum number of time frames is achieved.
11. Create a ring-shaped mask around the spot for measuring the local background intensity by subtracting the spot mask from a dilated version of the spot mask.
12. Measure mean intensities in the spot, the local background and the whole nucleus area in all channels and for all time frames. Additionally, measure the spot area (*EImage: computeFeatures.shape*).

13. Calculate the amounts of recruited fluorescent proteins in arbitrary units by multiplying the local-background-subtracted spot intensity by the spot area:

$$E(t) = (I_{\text{spot}} - I_{\text{background}}) \cdot A_{\text{spot}} \text{ (see Notes 11 and 12).}$$

14. Extract the individual times of acquisition t for each nucleus relative to the start of blue light illumination using the cycle number c , the grid position p , the total number of grid positions g , and the time it takes to once cycle over all grid positions d :

$$t = (c - 1) \cdot d + (p - 1) / g \cdot d \text{ (see Note 13).}$$

15. Save a table containing time, spot and background intensities and areas, as well as the spot mask. The result folder of the analysis at this point will contain a set of image series cropped around the tracked nucleus, the segmentation masks and a table with intensities and areas of the segmented regions for each cell.
16. Since cells have been selected only at one time point in the effector channel (GFP), a further selection step is necessary to sort out cells without tdMCP-tdTomato expression or incorrect segmentation or tracking. This is accomplished by annotating the image series of segmented cells in the RNA channel with the *NSSQ: annotateCells* script. Classify the cells as “g” (good; tdMCP-tdTomato expression, correct segmentation, tracking, and induction of transcription), “b” (bad; e.g., due to abnormal morphology, incorrect segmentation or tracking, or no tdMCP-tdTomato expression), “p” (prerecruitment; RNA production before TF recruitment), or “n” (good, but no visible induction of transcription over whole time course).
17. For averaging time courses of different cells (annotated as “good”) with the script provided, interpolate the integrated effector or RNA intensities at time points in the center of each cycle interval for each individual cell. Then average over all cells for each interpolated time point (see Note 14).

4 Notes

1. BLInCR is compatible with targeting a CIBN-fused localizer protein to a variety of nuclear binding sites [11]. For transcription induction both the *tetO* and the *lacO* repeats at the promoter in the U2OS 2-6-3 cell line can be used to recruit an activator protein. However, activation from the *tetO* sites is more efficient.
2. Regular white polystyrene foam boxes can be partly light permeable. To prevent premature activation, the denser black polystyrene foam boxes used for food delivery are

recommended. Furthermore, any light source of wavelengths below ~550 nm, for example, nearby computer screens, can trigger activation of the optogenetic system and should be switched off while the cells are not fully protected from light.

3. A variety of localizer, effector, and reader plasmids constructed in ref. 11 are available from Addgene (IDs #103797 to #103840).
4. To prevent premature activation by accidental light exposure as well as DNA replication problems, cells should be kept at conditions where the CIBN-TetR/rTetR constructs are present in the unbound state prior to the transcription activation experiments. Thus, during cell culturing, dox should be absent for reverse rTetR (DNA binding with dox) and present for TetR (DNA binding without dox).
5. Deletion of the TATA-box in the CMV promoter of tdMCP-tdTomato leads to lower expression levels, which results in a reduced nuclear background of unbound tdMCP molecules. Due to the high affinity of tdMCP, typical expression levels of around 0.1–1 μM as measured by fluorescence correlation spectroscopy are reached that are sufficient for saturating MS2 bindings sites on the reporter RNA [27].
6. The association and dissociation times of the PHR/CIBN and rTetR/*tetO* interactions must be considered when planning experiments. For rTetR the time for half-saturation of operator sites has been determined to be around 2 min for typical expression levels [8]. Thus, dox addition 10 min before the experiment start should be sufficient for saturated binding of rTetR. Previously, we have determined the time for half of the PHR molecules to dissociate from the *tetO* array to be 4.9 ± 0.8 min [11]. Thus, we recommend waiting for at least 15 min after imaging before adding dox to another well of the same slide since it may have been exposed to stray light. In this manner, no PHR fusion with the activator should be recruited to the promoter along with CIBN-rTetR before the actual start of the experiment. Alternatively, two slides can be used with one slide being stored in the dark while the other is imaged.
7. Light-induced recruitment can be heterogeneous between cells with different expression levels. Even though recruitment of PHR to CIBN is fast, expression levels of both PHR-activator and CIBN-rTetR need to be sufficient to saturate the *tetO* binding sites. Additionally, low blue light intensities during imaging can lead to slow recruitment kinetics in the minute range. In this case the experiment can be modified to include an initial light flash at higher intensity before the start of imaging to ensure complete conversion of PHR to its CIBN-interacting state. However, it should be noted that at high expression levels

and high blue light exposure PHR can undergo self-association into large assemblies of μm size [28].

8. Living cells typically move during an imaging period of 45–60 min. Thus, for the confocal microscopy experiments it might be necessary to adjust the field of view and the focus during the experiment.
9. To find and set the correct z -plane without inducing transcription, red transmission light illumination or use of appropriate filters is recommended. A red LED held above the slide can be used if red light illumination is not available at the microscope. In our experience, the reporter array is often located in the upper part of the nucleus (more distant from the bottom of the well). The nucleoli can be used to judge if a good focal plane has been selected.
10. The TurboReg plugin [26] applied for the analysis of confocal images uses intensity transformations prior to registering the images, leading to differences from the raw images. Since all images are recorded with the same laser intensities, the transformations should be similar for each time point. An alternative R-package for registration without intensity transformations is RNiftyReg from John Clayden (<https://github.com/jonclayden/RNiftyReg>), which is based on a previously described algorithm [29].
11. The background-subtracted integrated intensities in the spot are used as a quantitative readout for activator and reporter RNA accumulation. Different sizes of the segmented spot area do not affect this quantity as long as out-of-spot regions have the same intensity as the local background and will thus not contribute to the signal. For confocal imaging, photobleaching needs to be accounted for as described in Subheading 3.4.1. For widefield image series, normalization to the nuclear background intensity is not recommended. Background autofluorescence is much higher in widefield mode and will bleach with a different rate than the fluorescent protein. Furthermore, photobleaching is much less pronounced than for confocal images. The contribution of bleaching can be determined in time series of cells transfected with GFP-LacI for which a constant enrichment at the array is expected.
12. The nuclear background intensity is not uniform in a fluorescence widefield image due to the different z -extensions of the nucleus at its center and its edges. Therefore, the local background in a ring-shaped area around the spot is subtracted. Alternatively, a background intensity gradient can be subtracted as proposed by Ferguson and Larson [30]. Calculation of a background gradient image is implemented into the NSSQ package in the *tiltedPlane* function.

13. The time points of images are calculated from the number of imaged positions and the time it takes to cycle once over all positions. All positions will be exposed to light once the first position is imaged so that all positions share a common time point zero. The maximum time lag between the acquisition of two positions is determined by the cycle time. Care must be taken to interpolate intensity values at common time points, when averaging the recruitment time courses of cells at different positions. Time-lags should not exceed 3.5 min for sufficient time resolution of the dynamics and comparability of cells at different positions.
14. The single cell time traces of RNA production exhibit significant variations in the intensity of the signal. To some extent these can reflect differences in the size of reporter arrays integrated in the U2OS 2-6-3 cell line that arise from an inherent instability of these repeats. The latter is apparent from transfecting the cells with GFP-LacI, which reveals significant differences in spot size and intensity, and this signal can be used to quantitate the number of reporter genes in a given cell. Furthermore, the GFP-LacI signal can be exploited to quantify the noise in the spot intensity quantification that arises due to movements in *z*-direction or variations in spot segmentation.

Acknowledgments

We thank Pranas Grigaitis for help and the DKFZ light microscopy core facility for technical support. This work was supported by the Deutsche Forschungsgemeinschaft (DFG grant RI 1283/14-1 to K.R.) and the project ENHANCE within the NCT 3.0 program of the National Center for Tumor Diseases (NCT), Heidelberg.

References

1. Darzacq X, Yao J, Larson DR, Causse SZ, Bosanac L, de Turreis V, Ruda VM, Lionnet T, Zenklusen D, Guglielmi B, Tjian R, Singer RH (2009) Imaging transcription in living cells. *Annu Rev Biophys* 38:173–196. <https://doi.org/10.1146/annurev.biophys.050708.133728>
2. Martin RM, Rino J, Carvalho C, Kirchhausen T, Carmo-Fonseca M (2013) Live-cell visualization of pre-mRNA splicing with single-molecule sensitivity. *Cell Rep* 4 (6):1144–1155. <https://doi.org/10.1016/j.celrep.2013.08.013>
3. Cho WK, Jayanth N, English BP, Inoue T, Andrews JO, Conway W, Grimm JB, Spille JH, Lavis LD, Lionnet T, Cisse II (2016) RNA Polymerase II cluster dynamics predict mRNA output in living cells. *elife* 5:e13617. <https://doi.org/10.7554/eLife.13617>
4. Larson DR, Fritzsche C, Sun L, Meng X, Lawrence DS, Singer RH (2013) Direct observation of frequency modulated transcription in single cells using light activation. *elife* 2:e00750. <https://doi.org/10.7554/eLife.00750>
5. Chubb J, Trcek T, Shenoy S, Singer R (2006) Transcriptional pulsing of a developmental

- gene. *Curr Biol* 16(10):1018–1025. <https://doi.org/10.1016/j.cub.2006.03.092>
6. Bertrand E, Chartrand P, Schaefer M, Shenoy SM, Singer RH, Long RM (1998) Localization of ASH1 mRNA particles in living yeast. *Mol Cell* 2(4):437–445
 7. Darzacq X, Shav-Tal Y, de Turris V, Brody Y, Shenoy SM, Phair RD, Singer RH (2007) In vivo dynamics of RNA polymerase II transcription. *Nat Struct Mol Biol* 14(9):796–806. <https://doi.org/10.1038/nsmb1280>
 8. Normanno D, Boudarene L, Dugast-Darzacq-C, Chen J, Richter C, Proux F, Benichou O, Voituriez R, Darzacq X, Dahan M (2015) Probing the target search of DNA-binding proteins in mammalian cells using TetR as model searcher. *Nat Commun* 6:7357. <https://doi.org/10.1038/ncomms8357>
 9. Janicki SM, Tsukamoto T, Salghetti SE, Tansey WP, Sachidanandam R, Prasanth KV, Ried T, Shav-Tal Y, Bertrand E, Singer RH, Spector DL (2004) From silencing to gene expression: real-time analysis in single cells. *Cell* 116(5):683–698
 10. Kennedy MJ, Hughes RM, Peteya LA, Schwartz JW, Ehlers MD, Tucker CL (2010) Rapid blue-light-mediated induction of protein interactions in living cells. *Nat Methods* 7(12):973–975. <https://doi.org/10.1038/nmeth.1524>
 11. Rademacher A, Erdel F, Trojanowski J, Schumacher S, Rippe K (2017) Real-time observation of light-controlled transcription in living cells. *J Cell Sci* 130(24):4213–4224. <https://doi.org/10.1242/jcs.205534>
 12. Konermann S, Brigham MD, Trevino AE, Hsu PD, Heidenreich M, Cong L, Platt RJ, Scott DA, Church GM, Zhang F (2013) Optical control of mammalian endogenous transcription and epigenetic states. *Nature* 500(7463):472–476. <https://doi.org/10.1038/nature12466>
 13. Motta-Mena LB, Reade A, Mallory MJ, Glantz S, Weiner OD, Lynch KW, Gardner KH (2014) An optogenetic gene expression system with rapid activation and deactivation kinetics. *Nat Chem Biol* 10(3):196–202. <https://doi.org/10.1038/nchembio.1430>
 14. Rullan M, Benzinger D, Schmidt GW, Miliars-Argeitis A, Khammash M (2018) An Optogenetic platform for real-time, single-cell interrogation of stochastic transcriptional regulation. *Mol Cell* 70(4):745–756 e746. <https://doi.org/10.1016/j.molcel.2018.04.012>
 15. Polstein LR, Gersbach CA (2015) A light-inducible CRISPR-Cas9 system for control of endogenous gene activation. *Nat Chem Biol* 11(3):198–200. <https://doi.org/10.1038/nchembio.1753>
 16. R Core Team (2013) R: a language and environment for statistical computing. R Foundation for Statistical Computing, Vienna
 17. Soutoglou E, Misteli T (2008) Activation of the cellular DNA damage response in the absence of DNA lesions. *Science* 320(5882):1507–1510. <https://doi.org/10.1126/science.1159051>
 18. Bintu L, Yong J, Antebi YE, McCue K, Kazuki Y, Uno N, Oshimura M, Elowitz MB (2016) Dynamics of epigenetic regulation at the single-cell level. *Science* 351(6274):720–724. <https://doi.org/10.1126/science.aab2956>
 19. RStudio Team (2015) RStudio: integrated development for R. RStudio, Inc, Boston, MA
 20. Pau G, Fuchs F, Sklyar O, Boutros M, Huber W (2010) EBImage—an R package for image processing with applications to cellular phenotypes. *Bioinformatics* 26(7):979–981. <https://doi.org/10.1093/bioinformatics/btq046>
 21. Wickham H (2011) The split-apply-combine strategy for data analysis. *J Stat Softw* 40(1):1–29
 22. Wickham H (2016) ggplot2: elegant graphics for data analysis. Springer, New York
 23. Schindelin J, Arganda-Carreras I, Frise E, Kaynig V, Longair M, Pietzsch T, Preibisch S, Rueden C, Saalfeld S, Schmid B, Tinevez JY, White DJ, Hartenstein V, Eliceiri K, Tomancak P, Cardona A (2012) Fiji: an open-source platform for biological-image analysis. *Nat Methods* 9(7):676–682. <https://doi.org/10.1038/nmeth.2019>
 24. Schneider CA, Rasband WS, Eliceiri KW (2012) NIH image to ImageJ: 25 years of image analysis. *Nat Methods* 9(7):671–675
 25. Eck S, Worz S, Muller-Ott K, Hahn M, Biesdorf A, Schotta G, Rippe K, Rohr K (2016) A spherical harmonics intensity model for 3D segmentation and 3D shape analysis of heterochromatin foci. *Med Image Anal* 32:18–31. <https://doi.org/10.1016/j.media.2016.03.001>
 26. Thevenaz P, Ruttimann UE, Unser M (1998) A pyramid approach to subpixel registration based on intensity. *IEEE Trans Image Process* 7(1):27–41. <https://doi.org/10.1109/83.650848>
 27. Wu B, Chao JA, Singer RH (2012) Fluorescence fluctuation spectroscopy enables quantitative imaging of single mRNAs in living cells. *Biophys J* 102(12):2936–2944. <https://doi.org/10.1016/j.bpj.2012.05.017>
 28. Shin Y, Berry J, Pannucci N, Haataja MP, Toettcher JE, Brangwynne CP (2017) Spatio-temporal control of intracellular phase transitions using light-activated optodroplets. *Cell*

- 168(1–2):159–171 e114. <https://doi.org/10.1016/j.cell.2016.11.054>
29. Modat M, Cash DM, Daga P, Winston GP, Duncan JS, Ourselin S (2014) Global image registration using a symmetric block-matching approach. *J Med Imaging (Bellingham)* 1(2):024003. <https://doi.org/10.1117/1.JMI.1.2.024003>
30. Ferguson ML, Larson DR (2013) Measuring transcription dynamics in living cells using fluctuation analysis. In: Shav-Tal Y (ed) *imaging gene expression: methods and protocols*. Humana Press, New York, pp 47–60